

Intensified solvent extraction of L-tryptophan in small channels using D2EHPA

Haoyu Wang, Panagiota Angeli*

ThAMeS Multiphase, Department of Chemical Engineering, University College London,

Torrington Place, London WC1E 7JE, UK

**corresponding author: p.angeli@ucl.ac.uk*

Abstract

The continuous extraction of an amino acid, L-tryptophan, from aqueous solutions was studied in small channels with diameters of 0.5 mm and 2 mm. L-tryptophan was separated from nitric acid solutions into hexane using Di(2-ethylhexyl)phosphoric acid (D2EHPA) as extractant. It was found that the plug flow dominated in the flow pattern map at mixture velocities below 0.1 m/s and all organic phase volume fractions in the 0.5 mm channel, while it appeared at mixture velocities below 0.02 m/s and organic phase volume fractions below 60% in the 2 mm channel. During plug flow, the specific interfacial area increased with mixture velocity and acquired maximum values of 4432 and 1456 m²/m³ in the 0.5 and 2 mm channels respectively. Extraction efficiencies and percentage of up to 95% and 50% were reached in the 0.5 mm channel for residence times less 45s, while both values were about 5-10% less in the 2 mm channel. Mass transfer coefficients of up to 0.16 and 0.13 s⁻¹ were reached in the 0.5 mm and 2 mm channels respectively.

Keyword: Small channel; Liquid-liquid extraction; Intensification; Amino acid

Introduction

Liquid-liquid, or solvent, extraction (LLE) is one of the most important and efficient separation methods widely used in many industries. It is employed broadly in various processes including separation of metals, retrieval of biological compounds, such as proteins, enzymes, and amino acids, recovery and purification of biomolecules from fermented broth, industrial wastewater treatment, and reprocessing of spent nuclear fuel [1-10]. The separation is based on the solubilities of the compounds of interest in two immiscible liquids, an aqueous phase and an organic solvent. In particular, amino acids are an important class of compounds that have a variety of biological, industrial, and environmental applications, including food, animal feed additives, and in agriculture as plant nutrients [11-14]. The separation of amino acids plays an important role in many scientific and industrial fields. Amino acids contain an amino ($-\text{NH}_3^+$) and a carboxylate group ($-\text{COO}^-$), which result in their existence in acidic, basic, or zwitterion form depending on the pH value of the solution. These features make amino acids hydrophilic at all values of pH and therefore difficult to remove from aqueous solutions in conventional solvent extraction. To enhance the extractive potential of organic solvents, certain extractants, such as crown ether based extractant (18-crown-6, benzo-18-crown-6, dibenzo-18-crown-6, dicyclohexyl-18-crown-6) [15-20], cationic extractants Di(2-ethylhexyl)phosphoric acid (D2EHPA) [11, 21-26] and metal complexes (such as BINAP-metal, MeO-BIPHEP-metal, and SDP-metal) [27-31], are added in the organic phase. Crown ether based extractants and D2EHPA form stable hydrophobic complexes with the amino acids via hydrogen bonding and have long been used in their liquid-liquid extraction. For the extraction of amino acids, crown ethers are generally dissolved in chlorinated hydrocarbons or chloroform, while D2EHPA is used with hydrocarbons such as hexane, heptane and octane.

Metal complexes have also been tested in the liquid-liquid extraction process of amino acids very recently as chiral selectors. Similar to crown ether based extractants, metal complexes are dissolved in chlorinated hydrocarbons or chloroform.

The conventional equipment used in liquid-liquid extraction, such as mixer-settlers, packed, spray, pulsed and rotating disk columns, has many disadvantages, such as use of large solvent volumes, multistage extractions and long extraction times. [32-36] Moreover, the interfacial area related to the drop size in the conventional equipment, cannot be easily controlled. The drop size distributions are often broad and result in a wide range of times needed to complete the extraction. Non-uniform drop sizes result in varying extraction rates in the equipment. The extraction rate increases with decreasing drop size because the interfacial area is increased. However, with further decrease of the drop size the extraction rate decreases because the small drops behave as rigid spheres where molecular diffusion governs the mass transport [37, 38].

To overcome the drawbacks of the conventional equipment, process intensification (PI) which often involves small scale devices, such as small channels, can be applied in liquid-liquid extraction. Studies have shown that during multiphase flows in small channels, bubble/drop sizes are small and have narrow size distribution; large interfacial areas can thus be achieved [39-41]. In small channels, the interfacial and viscous forces dominate over gravity and result in regular patterns, such as plug flow, where elongated drops of one liquid (plugs), with diameter larger than the channel diameter, are separated by the continuous phase (slugs), while a thin film separates the plugs from the channel wall. Plug flows have been associated with improved mixing due to the circulations within the plugs and slugs [42-44], short diffusion distances because of the thin films [45] and large interfacial areas (ranging from

2760 to 8500 m²/m³ in channels with internal diameter smaller than 1 mm) [8, 46, 47], which increase mass transfer rates. Previous studies have shown that the efficiency and overall mass transfer coefficients of metal extractions, such as Eu(III), Ti, Pt(IV), and U(VI), in small channels could reach above 90% and 0.06 s⁻¹ respectively [8, 48-51].

There are currently no studies on the continuous extraction of amino acids in small channels with conventional organic solvents, despite the potentially significant improvements on mass transfer rates. In this paper, we report for the first time the continuous separation in small channels of L-tryptophan from an aqueous solution into an organic phase using D2EHPA as extractant. We present detailed flow pattern maps which indicate the range of flowrates where plug flow occurs, that enhances mass transfer. The effects of the flowrates of the two phases, the residence time, the channel size and the concentrations of the amino acid and the extractant on the extraction percentage and the mass transfer coefficients are investigated. The findings can be implemented for the design of intensified solvent extractions in small channels of other biomolecules.

Experimental set-up

Materials

Crown ethers and D2EHPA are commonly used as extractants for the separation of amino acids. However, crown ethers are usually dissolved in organic solvents such as chlorinated hydrocarbons or chloroform, which can be toxic. In this work Bis(2-ethylhexyl) phosphate (D2EHPA) was chosen, because it is chemically stable, has very low solubility in aqueous solutions, can be dissolved in less harmful hydrocarbon solvents, and is very effective in the extraction of many amino acids [25, 52-54]. The amino-acid, L-tryptophan ($\geq 98\%$ wt/wt purity,

molecular weight of 204.32 g/mol) and the extractant D2EHPA (97% wt/wt purity, molecular weight of 322.42 g/mol) were obtained from Sigma-Aldrich (UK) and used as received. The chemical structures of L-tryptophan and D2EHPA are shown in Fig. 1. The aqueous phase solution was prepared by dissolving the amino acid in deionised water and adjusting the pH value with 70% wt/wt nitric acid (HNO₃). In literature, various hydrocarbon solvents have been used for the extraction of amino acids, which showed no significant difference in the results. In the current work, hexane is selected as the organic solvent because of its low cost and the extremely low solubility of the amino acid in it. The organic phase solution was prepared by dissolving D2EHPA into hexane ($\geq 98.5\%$ wt/wt purity). Hexane and nitric acid were also purchased from Sigma-Aldrich (UK).

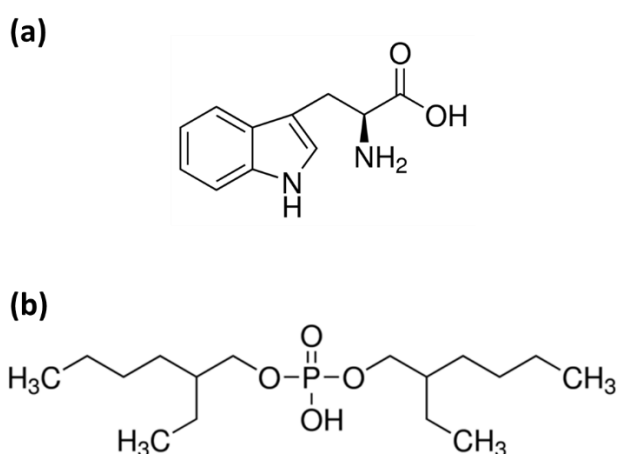


Figure 1. Chemical structure of (a) L-tryptophan and (b) D2EHPA.

Experimental setup for continuous extractions in small channels

The continuous flow experimental set-up is shown in Fig. 2a. The aqueous and organic phases, immiscible to each other, were injected separately by two high precision continuous syringe

pumps (Kd Scientific) via polytetrafluoroethylene (PTFE) tubing that had the same diameter (0.5 mm) and joined in a T-junction mixer (Fig. 2b) made of fluorinated ethylene propylene (FEP), where all side channels had the same diameter of 0.5 mm. After the T-junction, the mixture of the two-phases flowed through the main channel (made of PTFE with the diameter of 0.5 and 2 mm, which is hydrophobic and preferably wetted by the organic phase) and was separated in-line using a membrane-based flow separator (SEP-10 Zaiput, Flow Technologies). The membrane used was made of PTFE (part number IL-900-S10) and was hydrophobic, thus allowing the organic phase to permeate it while the aqueous phase was retained.

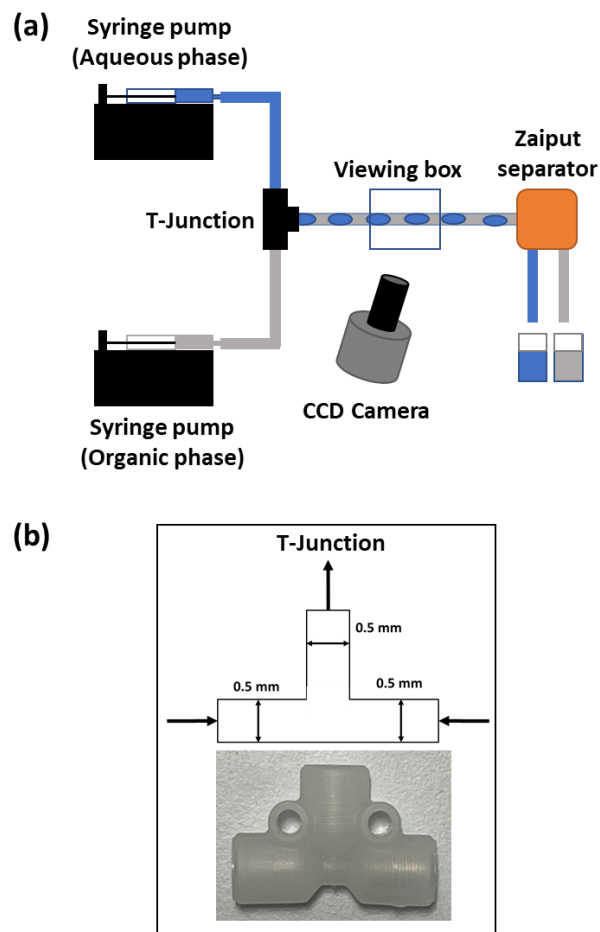


Figure 2. (a) Experimental set up for the continuous flow experiments in small channels. (b) Schematic and photograph of the T-junction.

Experiment procedure

The extraction experiments were carried out at atmospheric pressure and room temperature ($T= 298\text{K}$). Amino acid solutions in the aqueous phase were initially prepared for the equilibrium studies with concentrations in the range between 0.00096 and 0.0096 M, as was verified by measurements in a Cary-60 high-end UV-Vis spectrometer (Agilent UK). Nitric acid was added into the aqueous phase solutions to keep the pH value constant at $\text{pH}=1$. The concentration of D2EHPA in the organic phase varied from 0.005 to 1.663 M, which was in a similar range to previous batch extraction studies for the same mixtures.

The equilibrium experiments were carried out to obtain the partition coefficients of the amino acid between the two phases. For these experiments, equal volumes of the aqueous and the organic phase solutions (5 mL) were added in stoppered vessels and then mixed with a magnetic stirrer at constant rotational speed for 1 hour. The aqueous phase was removed from the vessel every 5 mins for the concentration measurements with the UV-Vis at 280 nm. The same amount of the organic phase solution was also removed from the vessel to keep the volumes of the two phases equal. The concentration of amino acid in the aqueous phase initially decreased but after about 40 minutes it reached a constant value which was taken as the equilibrium concentration. The distribution coefficient (D) was then calculated according to the equation

$$D = \frac{C_{aq,ini} - C_{aq,eq^*}}{C_{aq,eq^*}} \quad (1)$$

where $C_{aq,ini}$ and C_{aq,eq^*} are the initial and final concentrations of amino acid in the aqueous phase.

For the continuous extraction experiments, two different channels with diameters 0.5 and 2 mm were used. The two phases were injected at the same volume flow rate in the small channels using the syringe pumps. The organic phase was fed initially in the channel as the continuous phase in contact with the channel wall, while the aqueous phase was introduced later and became the dispersed phase. Initially, flow pattern maps were constructed for both channels to identify the conditions that resulted in plug flow for mixture velocities ranging between 0.0001 m/s and 1 m/s and volume flowrate fractions of the organic phase varying between 10% and 90%. For the extraction experiments the lengths of the test channels varied between 15 to 75 cm to obtain different residence times at certain mixture velocities. The phases were separated at the outlet by the Zaiput separator and collected individually; the amino acid concentration in the aqueous phase was measured using the UV-Vis instrument.

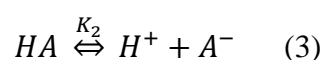
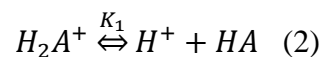
The flow patterns and the characteristics of the plug flow in the main channel, were studied with a Photron Fastcam-ultima high speed camera at frame rates between 1000-5000Hz. To reduce optical reflections, the main channel was enclosed in a visualization box filled with water that has refractive index (1.33) similar to that of the channel wall (1.35). The resolutions of the images are 88 and 98 px/mm for the 0.5 and 2 mm channels. As the resolutions are not high enough for the measurement of film thickness, this was calculated from correlations (see next section). In plug flow, the plug length was determined by averaging over 10 images with low values of standard deviation up to 3%.

Results and discussion

Equilibrium studies

At neutral pH value, the amino acid is a zwitterion with a carboxylic group and an amino group.

Two dissociation equilibria exist in aqueous solutions:

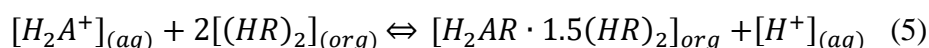


where H_2A^+ , HA , A^- is the cationic, neutral, and anionic form of the amino acid, respectively.

Only the cationic form of the amino acids, depending on the pH of the aqueous solution, can be extracted using D2EHPA. Since previous equilibrium studies have been conducted for pH < 3.0 [24, 25, 55], the pH value in the current work is set to 1 with nitric acid. The dissociation constants for the above equations are given below:

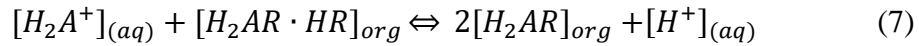
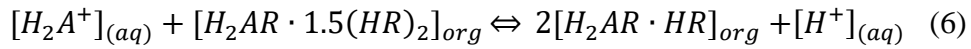
$$K_1 = \frac{[H^+][HA]}{[H_2A^+]} \quad K_2 = \frac{[H^+][A^-]}{[HA]} \quad (4)$$

In aqueous solutions, the pK_1 and pK_2 of L-Trp are 2.38 and 9.38 respectively [56]. During extraction, D2EHPA and the cationic amino acid form a complex, which diffuses into the organic phase. There are three types of complexes forming based on the concentration of the amino acid during extraction. At low L-Trp concentrations (less than 5.0 mM), only one form of the complex, $H_2AR \cdot 1.5(HR)_2$ appears in the solution [25, 53], as expressed by:



where $(HR)_2$ is the D2EHPA dimer.

Two additional complexes, $H_2AR \cdot HR$ and H_2AR , co-exist with the previous one at higher concentrations of the amino acid as shown below:



At low L-Trp concentration, one molecule of cationic L-Trp is extracted by four monomeric D2EHPA molecules, while the other complexes, $H_2AR \cdot HR$ and H_2AR , at higher amino acid concentrations are formed with less extractant molecules. It has been suggested that an increase in the D2EHPA concentration in the organic phase increases the extraction of the amino acid from the aqueous phase [25]. Thus, in the current studies a concentration ratio between L-Trp and D2EHPA of 1:1 to 1:10 was chosen to cover the possible ratios suggested by the kinetics of the extraction and the increase of extraction at high D2EHPA concentrations, as suggested by the literature.

The distribution coefficients obtained (Equation (1)) are shown in Fig. 3. At a constant total L-Trp concentration, the equilibrium concentration in the aqueous phase decreases with increasing D2EHPA concentration, while the distribution coefficient increases. The equilibrium results in Fig. 3 agree with previous research [25]. In the following continuous extractions in the small channels, concentrations of D2EHPA of 0.0096 M and 0.096 M are selected to extract 0.0096 M amino acid from the aqueous phase solution, which correspond to concentration ratios between amino acid and extractant of 1:1 and 1:10.

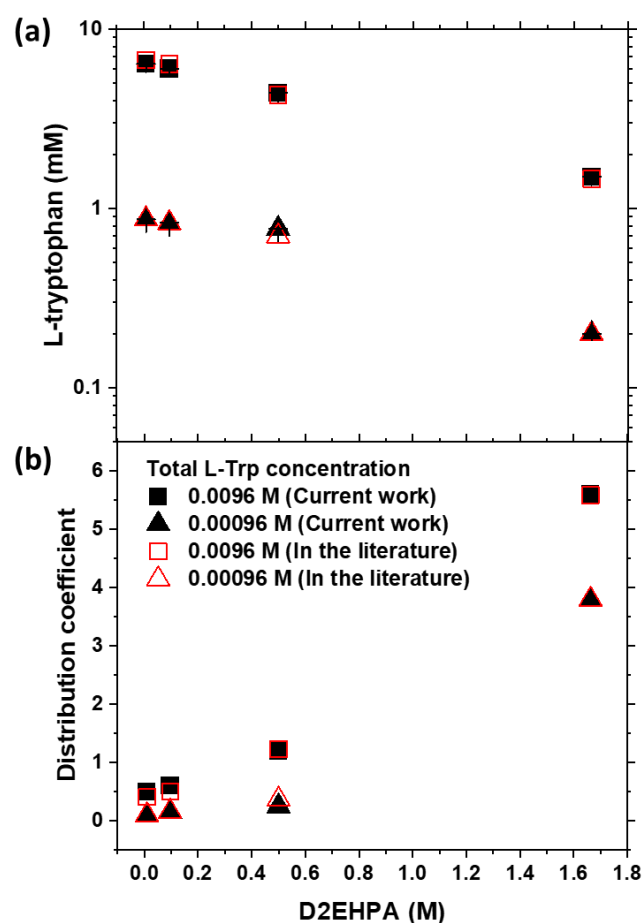


Figure 3. (a) L-Trp concentration in the aqueous phase at equilibrium for different concentrations of the extractant D2EHPA. (b) Distribution coefficients at different concentrations of the extractant. Black symbols are results from the current work, while red ones are literature data [25].

Flow patterns in the small channels

The characteristics of the flow patterns in the small channels can affect the extraction process. The flow pattern map for the flow of water and hexane in the 0.5 mm channel, is shown in Fig. 4. The extraction system where very small amounts of amino acid are present in the aqueous phase (<0.2% wt/wt) and of extractant in hexane (<3% wt/wt), have very similar

properties (interfacial tension: ~ 41 mN/m [57, 58]; density: 0.668 g/cm³, measured with bench scale and Fisherbrand pipettes at 25 °C) to those of the water-hexane system (interfacial tension: ~ 43 mN/m [59]; density: 0.66 g/cm³), and the patterns would be the same. In the same map, the boundary between plug flow and the other patterns for the 2mm channel is also shown. The Bond numbers ($B_o = gd^2(\rho_A - \rho_O)/\sigma$, where g is the gravitational acceleration, d is the diameter of the channel, ρ_A and ρ_O are the density of the aqueous and organic phases respectively, σ : is the interfacial tension) were calculated and were found equal to 0.0196 and 0.315 for the 0.5 mm and 2 mm channels, respectively, using the interfacial tension between the organic and aqueous phase. The values are below 0.88 which indicates that the gravitational forces are not significant and interfacial forces dominate [60, 61]. From the various patterns that can form, plug flow is preferred for mass transfer because of its regular characteristics, the large interfacial areas and the enhanced mixing [62]. As can be seen in Fig. 4, plug flow is the dominant pattern in the 0.5 mm channel for all phase flowrate fractions tested and mixture velocities below 0.1 m/s. In the 2 mm channel, plug flow appears at lower mixture velocities (below 0.02 m/s) and organic phase flowrate fractions smaller than 60% . The length of the plugs decreased with increasing mixture velocity as shown in Fig. 5. The shape of the plugs resembled that of a capsule. The specific interfacial area α_p can be calculated based on $\alpha_p = SA_p/V_{TU}$, where SA_p is the surface area of the plug and V_{TU} is the total volume of the unit cell, which includes a plug and a continuous phase slug. For the calculation, the front and back ends of the plug are considered as hemispheres and the section in between them is treated as a cylinder. The diameter of the cylinder is taken equal to the channel diameter minus the film thickness, δ , that separates the plug from the channel wall. The film thickness is calculated from $2\delta/d = 0.35Ca^{0.354}We^{0.097}$ [63], where Ca is the Capillary number ($\frac{\mu_O U}{\sigma}$, μ_O : viscosity of the organic

phase, U is the mixture velocity) and We is the Weber number ($\frac{\rho U^2 d}{\sigma}$, ρ is the density of the mixture). As shown in Fig. 5, the specific interfacial area increases with increasing mixture velocity. The Ca and We values in plug flow are below 10^{-3} and 1, respectively, indicating that the interfacial tension forces dominate over the viscous and inertial ones, and give the plugs their regular shape. The subsequent extraction studies were carried out at 50% phase volume fraction.

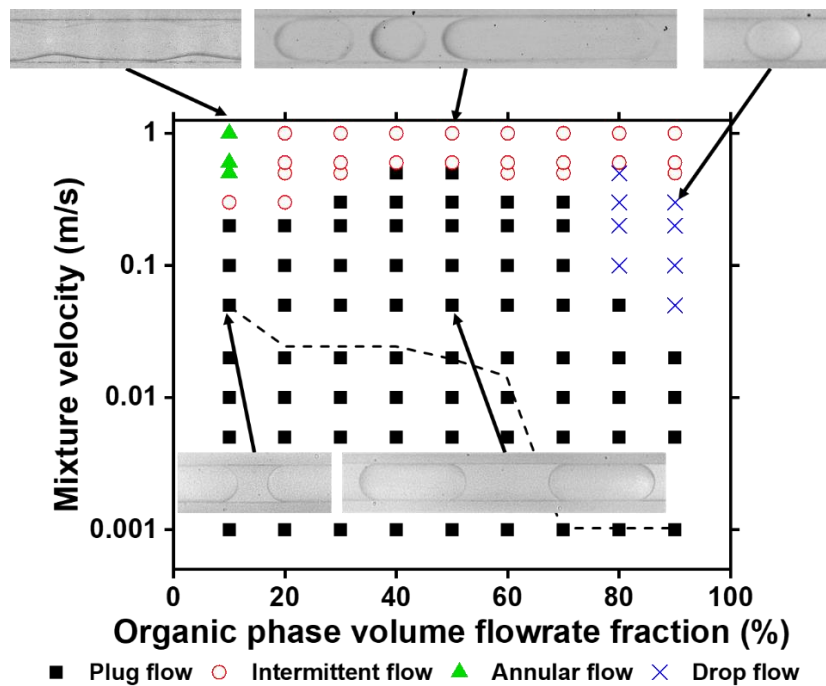


Figure 4. Flow pattern map for the flow of water and hexane. Symbols: flow patterns in the 0.5 mm channel; dashed line: boundary of plug flow in the 2 mm channel.

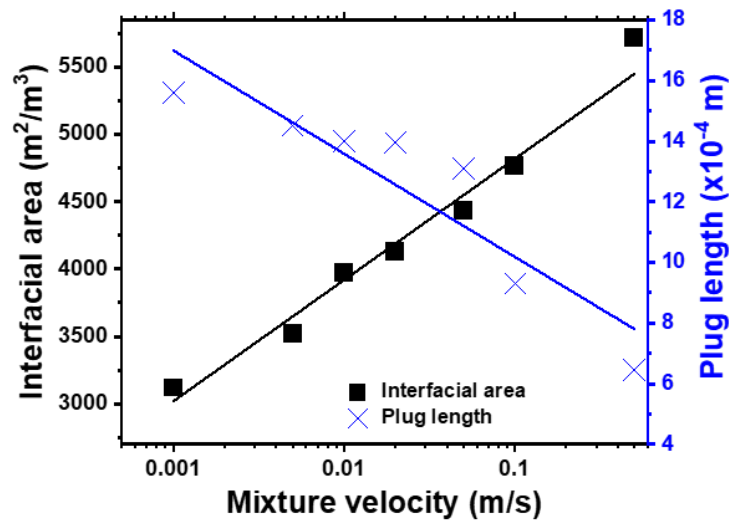


Figure 5. Plug length (black squares) and specific interfacial area (blue crosses) at different mixture velocities for the 0.5 mm channel.

The plug flow changed into intermittent flow with increasing mixture velocity, which is characterised by dispersed plugs with varying sizes. The transition depended on the channel size and the organic phase volume fraction and occurred at mixture velocities of around 0.3 m/s in the 0.5 mm channel, and at around 0.02 m/s in the 2 mm channel. Drop flow, where the dispersed phase has length equal to or smaller than the diameter of the channel, appeared at increasing organic flowrate fraction (above 0.7 in both channel sizes).

Continuous flow extractions in small channels

The continuous extractions in the small channels were carried out during plug flow at equal volumetric flow rates of the organic and the aqueous phases. The extraction efficiency ($E_{ff}\%$), extraction percentage ($E\%$) and the overall mass transfer coefficient ($k_L a$) were calculated using equations (8) to (10), respectively [64]:

$$Eff\% = \frac{C_{aq,in} - C_{aq,fin}}{C_{aq,ini} - C_{aq,eq^*}} \quad (8)$$

$$E\% = \frac{C_{aq,ini} - C_{aq,fin}}{C_{aq,ini}} \quad (9)$$

$$k_L a = \frac{1}{\tau} \ln \left(\frac{C_{aq,eq^*} - C_{aq,fin}}{C_{aq,eq^*} - C_{aq,in}} \right) \quad (10)$$

where $C_{aq,fin}$ is the final concentration of L-Trp in the aqueous phase at the outlet of the channel.

To isolate the effect of the mixture velocity on mass transfer, the channel length was varied with the mixture velocity to ensure that the residence time remained the same. In the 0.5 mm channel, the mixture velocity ranged from 0.01 to 0.05 m/s and the channel length increased appropriately from 15 to 75 cm which resulted in a resident time of 15 s, while in the 2 mm channel the mixture velocity varied between 0.01 and 0.04 m/s and the channel length ranged from 15 to 60 cm resulting in the same residence time.

As can be seen from Fig. 6, with increasing mixture velocity the extraction efficiency and percentage increase until about 95% and 50%, respectively. With increasing mixture velocity, the plug length decreases as shown in Fig 5. In the 0.5 mm channel, the plug length reduces from 1.4 mm at 0.01 m/s to 1.3 mm at 0.05 m/s. The circulation time within the plugs, defined as the average time to displace material from one to the other end of the plug, decreases as the plug length decreases at high mixture velocities [42]. Moreover, the decrease in plug length with increasing mixture velocity, leads to an increase of the specific interfacial area from 3968 to 4432 m²/m³ when mixture velocity increases from 0.01 m/s to 0.05 m/s, respectively. Both the decrease of circulation time and the increase of specific interfacial area result in better mass transfer with increasing mixture velocity.

The size of the channel has also an effect on the extraction efficiency. As shown in Fig. 6(a), the average efficiency in the 2 mm channel was about 5% lower than in the 0.5 mm channel, which is related to the decrease of the specific interfacial area with the increase of the channel diameter. At the mixture velocity of 0.01 m/s, the specific interfacial areas in the 0.5 and 2 mm channels are 3968 and 1253 m²/m³ respectively.

The effect of channel size and mixture velocity on the overall mass transfer coefficients, $k_L a$, is shown in Fig. 7. The mass transfer coefficients are reduced in the 2 mm channel compared to the 0.5 mm one, which is attributed to more intense mixing and increased specific interfacial area in the small channel sizes. They are also increased with the mixture velocity in both channels. As discussed above, the specific interfacial area in the 0.5 mm channel is 3968 m²/m³ at 0.01 m/s while the values in equipment such as packed columns and mixer-settlers, are less than 250 and 1000 m²/m³ respectively [65, 66].

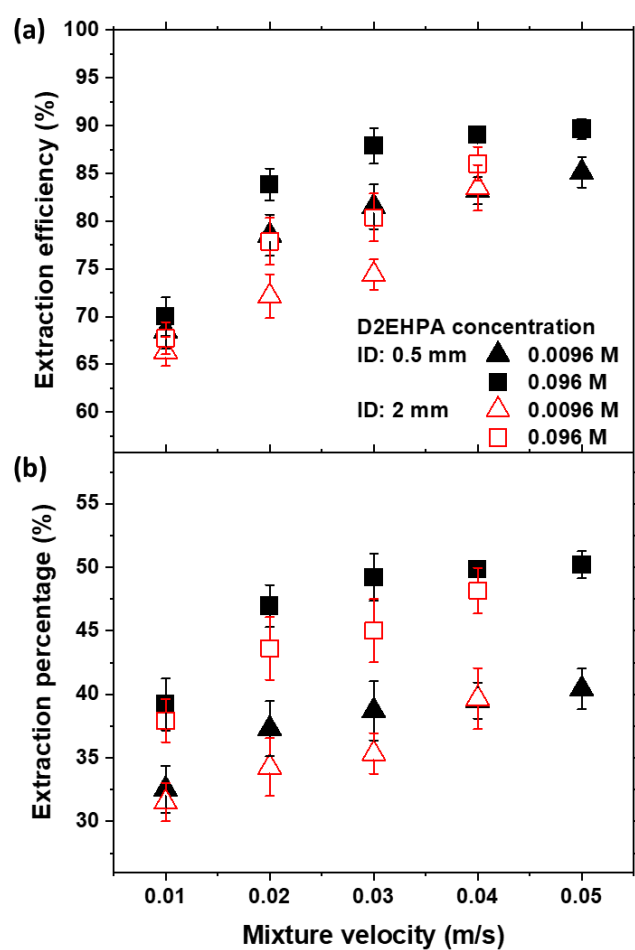


Figure 6. Effect of mixture velocity on (a) extraction efficiency and (b) percentage of extraction in the 0.5 mm and in the 2 mm channels. The channel length varies from 15 to 75 cm to ensure constant residence time equal to 15 s. Black and red symbols are the results in the 0.5 and 2 mm channels respectively. The concentrations of D2EHPA in hexane are 0.0096 M (triangle shapes) and 0.096 M (square shapes).

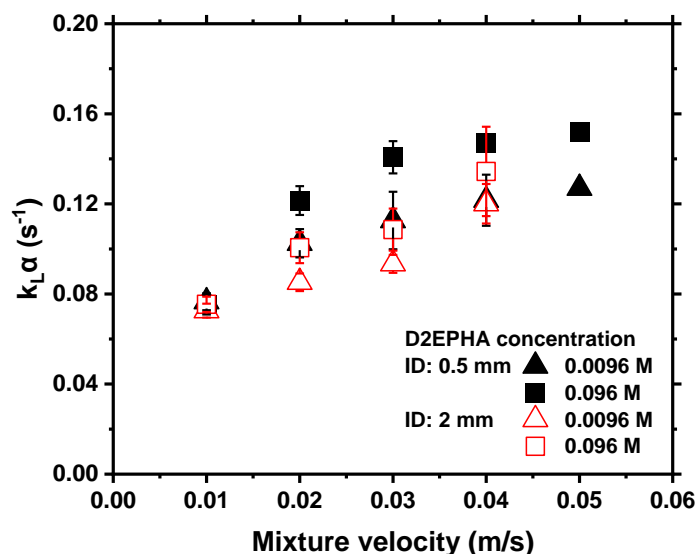


Figure 7. Overall mass transfer coefficient against mixture velocity in the 0.5 mm and 2 mm channels. The channel length varies from 15 to 75 cm to ensure constant residence equal to 15 s. Black and red symbols are the results in the 0.5 and 2 mm channels respectively. The concentrations of D2EHPA in hexane are 0.0096 M (triangle shapes) and 0.096 M (square shapes).

The effect of residence time on extraction efficiency and percentage can be seen in Fig. 8. To maintain the plug length, the mixture velocity was kept constant at 0.01m/s while the channel length varied from 15 to 60 cm accordingly. As it can be seen, the extraction efficiency increases with increasing residence time in both channel sizes. In the 0.5 mm channel, the extraction efficiency and percentage can reach, respectively, above 90% and 50% in 45 s at all extractant concentrations. The results are generally lower in the 2mm channel compared to the 0.5 mm one, with only one case (at the residence time of 30 s) with low extractant concentration in the 2 mm channel having the same efficiency and extraction percentage as in the 0.5 mm channel. The average extraction efficiency is lower in the 2 mm channel by about 6%, compared to the 0.5 mm one.

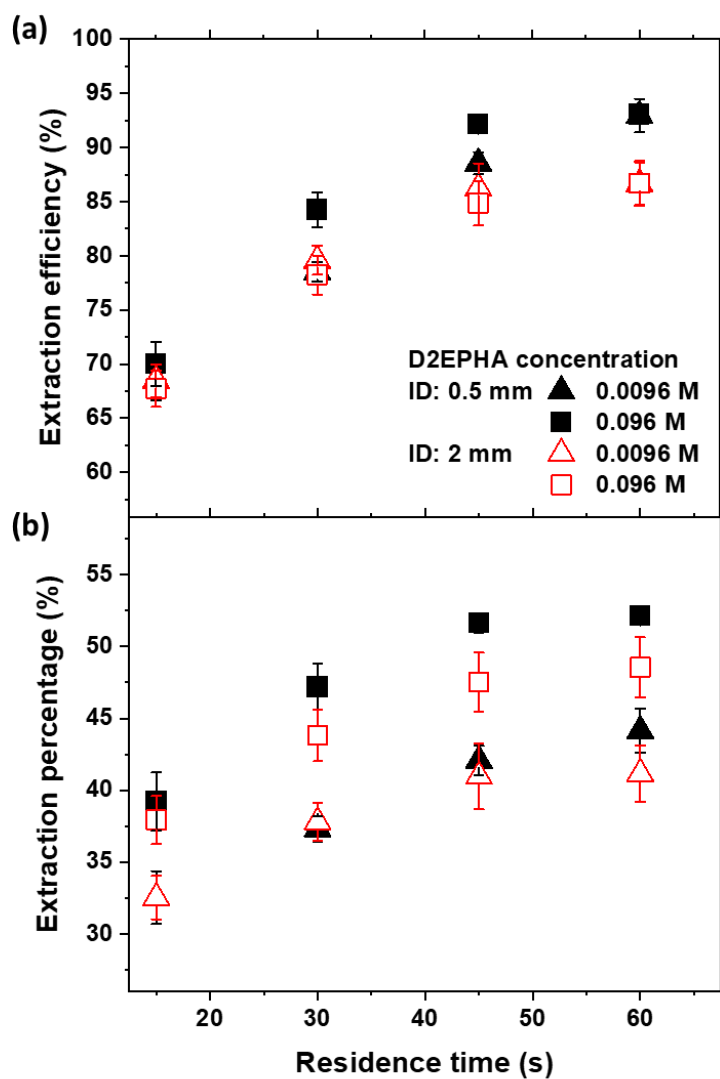


Figure 8. Effect of residence time on the extraction efficiency and percentage extraction of the amino acid in the 0.5 and 2 mm channels. The mixture velocity is kept constant at 0.01 m/s while the channel length varies from 15 to 60 cm. Black and red symbols are the results in 0.5 and 2 mm channel respectively. The concentrations of D2EHPA in hexane are 0.0096 M (triangle shapes) and 0.096 M (square shapes).

The overall mass transfer coefficients at constant mixture velocity decreased with increasing residence time (Fig. 9). Initially the decrease is large, but it becomes less prominent as the residence time increases. At the channel inlet after the T-junction, where the two phases first join, there is intense mixing and newly formed interfaces, while the concentration difference between the organic and aqueous phases is large, leading to enhanced mass transfer. Beyond the T-junction, fully developed plugs, that do not change in length, propagate further downstream in the channel while the concentration difference between the two phases decreases, resulting in small changes in $k_L a$. The mass transfer coefficients for the different extractant concentrations in Fig. 9 are close to each other. This is probably due to the mixture velocity (0.01 m/s) used to observe the effect of residence time on the mass transfer coefficient. As can be seen in Figure 6 (a) and Figure 7, the extraction efficiencies and $k_L a$ for the two different concentrations of the extractant at this mixture velocity (0.01 m/s) are all very close, in accordance with the results in Figure 9.

From the overall mass transfer coefficient, $k_L a$ and the specific interfacial area, k_L can be estimated. For the 0.5 and 2 mm channels, k_L ranges in $1.9 - 3.4 \times 10^{-5} \text{ m s}^{-1}$ and $5.8 - 9.3 \times 10^{-5} \text{ m s}^{-1}$ respectively. This parameter can then be used at other systems, where the specific interfacial area values are different.

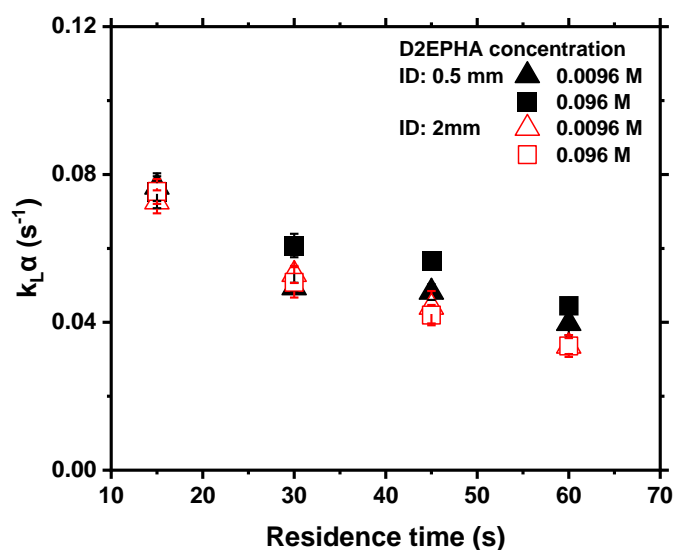


Figure 9. Effect of residence time on the overall mass transfer coefficient in the 0.5 and 2 mm channels. The mixture velocity is kept constant at 0.01 m/s while the channel length varies from 15 to 60 cm. Black and red symbols are the results in the 0.5 and 2 mm channels respectively. The concentrations of D2EHPA in the hexane are 0.0096 M (triangle shapes) and 0.096 M (square shapes).

Conclusions

In this paper we demonstrated the ability of small channels in intensifying the liquid-liquid extraction of the amino acid L-tryptophan from aqueous solutions into an organic solvent with D2EHPA as extractant.

The continuous extraction experiments were carried out in small channels with diameters 0.5 mm and 2 mm. Flow pattern maps of the organic and aqueous phase mixtures in both channels were obtained, which can be used as a guide for the selection of conditions resulting

in plug flow in similar systems. The largest specific interfacial areas of 4432 and 1456 m²/m³ respectively for the 0.5 and 2 mm channels, were obtained at the highest velocity used of 0.05 m/s. In general, the extraction percentage and extraction efficiencies increased with increasing residence time and with increasing mixture velocities for the same residence time and were generally lower in the 2 mm channel compared to the 0.5 mm one. The mass transfer coefficients also increased with the mixture velocity but decreased with the residence time.

The above extractions were achieved in residence times less than 1 min, which are much shorter than those used in mixer settlers and liquid-liquid extraction columns [25, 32, 34, 67]. The maximum mass transfer coefficient achieved in the current small channel systems is around 0.16 s⁻¹, while it is less than 0.1 s⁻¹ in both stirred batch vessel systems and extraction columns [25, 65, 68]. The results demonstrate the extraction of amino acids such as L-tryptophan can be intensified in small channels. The findings can be used to guide the design of small channel continuous separation systems for other amino acids or more generally biomolecules including enzymes and proteins.

References

1. de Lemos, L.R., I.J.B. Santos, G.D. Rodrigues, L.H.M. da Silva, and M.C.H. da Silva, *Copper recovery from ore by liquid-liquid extraction using aqueous two-phase system*. Journal of Hazardous Materials, 2012. **237-238**: p. 209-214.
2. Eccles, H., *Nuclear fuel cycle technologies -sustainable in the twenty first century*. Solvent Extraction and Ion Exchange, 2000. **18(4)**: p. 633-654.
3. Goklen, K.E. and T.A. Hatton, *Liquid-Liquid Extraction of Low Molecular-Weight Proteins by Selective Solubilization in Reversed Micelles*. Separation Science and Technology, 1987. **22(2-3)**: p. 831-841.
4. Huddleston, J., A. Veide, K. Köhler, J. Flanagan, S.-O. Enfors, and A. Lyddiatt, *The molecular basis of partitioning in aqueous two-phase systems*. Trends in Biotechnology, 1991. **9(1)**: p. 381-388.
5. Pires, M.J., M.R. Aires-Barros, and J.M.S. Cabral, *Liquid-Liquid Extraction of Proteins with Reversed Micelles*. Biotechnology Progress, 1996. **12(3)**: p. 290-301.

6. dos Santos, N.V., V. de Carvalho Santos-Ebinuma, A. Pessoa Junior, and J.F.B. Pereira, *Liquid–liquid extraction of biopharmaceuticals from fermented broth: trends and future prospects*. Journal of Chemical Technology & Biotechnology, 2018. **93**(7): p. 1845-1863.
7. Pedersen, M.E., J. Østergaard, and H. Jensen, *In-Solution IgG Titer Determination in Fermentation Broth Using Affibodies and Flow-Induced Dispersion Analysis*. ACS Omega, 2020. **5**(18): p. 10519-10524.
8. Li, Q. and P. Angeli, *Intensified Eu(III) extraction using ionic liquids in small channels*. Chemical Engineering Science, 2016. **143**: p. 276-286.
9. Tsaoulidis, D., V. Dore, P. Angeli, N.V. Plechkova, and K.R. Seddon, *Extraction of dioxouranium(VI) in small channels using ionic liquids*. Chemical Engineering Research and Design, 2013. **91**(4): p. 681-687.
10. Tsaoulidis, D., V. Dore, P. Angeli, N.V. Plechkova, and K.R. Seddon, *Dioxouranium(VI) extraction in microchannels using ionic liquids*. Chemical Engineering Journal, 2013. **227**: p. 151-157.
11. Juang, R.-S. and Y.-Y. Wang, *Amino acid separation with D2EHPA by solvent extraction and liquid surfactant membranes*. Journal of Membrane Science, 2002. **207**(2): p. 241-252.
12. Smirnova, S.V., I.I. Torocheshnikova, A.A. Formanovsky, and I.V. Pletnev, *Solvent extraction of amino acids into a room temperature ionic liquid with dicyclohexano-18-crown-6*. Analytical and Bioanalytical Chemistry, 2004. **378**(5): p. 1369-1375.
13. Huaxi, L., L. Zhuo, Y. Jingmei, L. Changping, C. Yansheng, L. Qingshan, Z. Xiuling, and W.-B. Urs, *Liquid–liquid extraction process of amino acids by a new amide-based functionalized ionic liquid*. Green Chemistry, 2012. **14**(6): p. 1721-1727.
14. Bremner, J.M., *Amino-acids in Soil*. Nature, 1950. **165**(4192): p. 367-367.
15. Noguchi, H., N. Yoshio, K. Kawahara, H. Nakamura, and M. Nagamatsu, *Application of Crown Ether to Chemical Analysis. III. Extraction of Amines with Crown Ether*. Analytical Letters, 1980. **13**(4): p. 271-282.
16. Hideyuki, N., N. Hiroyoshi, N. Masatoshi, and Y. Masaki, *The Solvent Extration of Amino Acids with Crown Ether*. Bulletin of the Chemical Society of Japan, 1982. **55**(1): p. 156-158.
17. Buschmann, H.-J., L. Mutihac, and R. Mutihac, *Physicochemical Parameters of the Transport of Amines and Amino Acids through Liquid Membranes by Macrocyclic Ligands*. Separation Science and Technology, 1999. **34**(2): p. 331-341.
18. Kai, C., T. Oshima, and Y. Baba, *Enhanced Extraction of Amino Compounds Using Dicyclohexyl-18-crown-6 as a Ligand in an Aqueous Two-phase System*. Solvent Extraction Research and Development, Japan, 2010. **17**: p. 83-93.
19. Mutihac, L., D.O. Popescu, and R.-I. Stefan, *Solvent Extraction of Amino Acids With Crown Ethers and Cryptand 222*. Analytical Letters, 1995. **28**(5): p. 835-843.
20. Zarna, N., T. Constantinescu, H. Caldaru, A. Caragheorgheopol, G. Stanciuc, A.T. Balaban, K. Laihla, and E. Kolehmainen, *Hydrophobic supramolecular complexes of various cations with 18-crown-6 as the ligand and N-methoxy-picramide as the anion pair in a water/methylene chloride two-phase system: complexes with α -amino acids, their characteristics and conditions for formation*. Supramolecular Science, 1995. **2**(1): p. 37-40.
21. Bai, H., K. Guo, X. Chen, Z. Chang, and D. Li, *Reactive extraction of L-valine with di(2-ethylhexyl) phosphate acid*. Journal of Chemical Technology & Biotechnology, 2016. **91**(12): p. 3096-3102.
22. Lin, S.-H., C.-N. Chen, and R.-S. Juang, *Extraction equilibria and separation of phenylalanine and aspartic acid from water with di(2-ethylhexyl)phosphoric acid*. Journal of Chemical Technology & Biotechnology, 2006. **81**(3): p. 406-412.
23. Liu, Y.-S., Y.-Y. Dai, and W. Jia-Ding, *Distribution Behavior of L-Phenylalanine by Extraction with Di(2-Ethylhexyl) Phosphoric Acid*. Separation Science and Technology, 1999. **34**(11): p. 2165-2176.

24. Liu, Y.S., Y.Y. Dai, and J.D. Wang, *Distribution Behavior of L-Tryptophane by Extraction with Di(2-ethylhexyl) Phosphoric Acid*. Separation Science and Technology, 2000. **35**(9): p. 1439-1454.
25. Shi, Q.-H., Y. Sun, L. Liu, and S. Bai, *Distribution Behavior of Amino Acid by Extraction with Di(2-ethylhexyl) Phosphoric Acid*. Separation Science and Technology, 1997. **32**(12): p. 2051-2067.
26. Wieczorek, P., J.Å. Jönsson, and L. Mathiasson, *Concentration of amino acids using supported liquid membranes with di-2-ethylhexyl phosphoric acid as a carrier*. Analytica Chimica Acta, 1997. **346**(2): p. 191-197.
27. Liu, J.-J., G.-H. Wu, K.-W. Tang, X. Liu, and P.-L. Zhang, *Equilibrium of chiral extraction of 4-nitro-d,l-phenylalanine with BINAP metal complexes*. Chemical Papers, 2014. **68**(1): p. 80-89.
28. Verkuil, B.J.V., A.J. Minnaard, J.G. de Vries, and B.L. Feringa, *Chiral Separation of Underivatized Amino Acids by Reactive Extraction with Palladium–BINAP Complexes*. The Journal of Organic Chemistry, 2009. **74**(17): p. 6526-6533.
29. Liu, X., Y. Ma, T. Cao, D. Tan, X. Wei, J. Yang, and L. Yu, *Enantioselective liquid-liquid extraction of amino acid enantiomers using (S)-MeO-BIPHEP-metal complexes as chiral extractants*. Separation and Purification Technology, 2019. **211**: p. 189-197.
30. Liu, X., Y. Ma, T. Cao, S.-p. Jiang, and P.-y. Yang, *Chiral extraction of amino acid enantiomers using (S)-SEGPHOS-metal complexes as extractants*. Chemical Papers, 2020. **74**(4): p. 1229-1239.
31. Tang, K., T. Fu, and P. Zhang, *Equilibrium Studies on Enantioselective Liquid–Liquid Extraction of Phenylalanine Enantiomers Using BINAP–Metal Complexes*. Journal of Chemical & Engineering Data, 2012. **57**(12): p. 3628-3635.
32. Wichterlová, J. and V. Rod, *Dynamic behaviour of the mixer–settler cascade. Extractive separation of the rare earths*. Chemical Engineering Science, 1999. **54**(18): p. 4041-4051.
33. Rezamohammadi, A., H. Bahmanyar, M. Sattari Najafabadi, and M. Ghafouri Rouzbahani, *Investigation of characteristic velocity in a pulsed packed column in the presence of SiO₂ nanoparticles*. Chemical Engineering Research and Design, 2015. **94**: p. 494-500.
34. Ashrafmansouri, S.-S. and M. Nasr Esfahany, *The influence of silica nanoparticles on hydrodynamics and mass transfer in spray liquid–liquid extraction column*. Separation and Purification Technology, 2015. **151**: p. 74-81.
35. Roozbahani, M.A.G., M.S. Najafabadi, K.N.H. Abadi, and H. Bahmanyar, *Simultaneous Investigation of the Effect of Nanoparticles and Mass Transfer Direction on Static and Dynamic Holdup in Pulsed-Sieve Liquid–Liquid Extraction Columns*. Chemical Engineering Communications, 2015. **202**(11): p. 1468-1477.
36. Wang, H., A. Mustaffar, A.N. Phan, V. Zivkovic, D. Reay, R. Law, and K. Boodhoo, *A review of process intensification applied to solids handling*. Chemical Engineering and Processing: Process Intensification, 2017. **118**: p. 78-107.
37. Chakraborty, M., C. Bhattacharya, and S. Datta, *Effect of drop size distribution on mass transfer analysis of the extraction of nickel(II) by emulsion liquid membrane*. Colloids and Surfaces A: Physicochemical and Engineering Aspects, 2003. **224**(1): p. 65-74.
38. Torab-Mostaedi, M., J. Safdari, M.A. Moosavian, and M.G. Maragheh, *Stage efficiency of Hanson mixer-settler extraction column*. Chemical Engineering and Processing: Process Intensification, 2009. **48**(1): p. 224-228.
39. Górak, A. and A. Stankiewicz, *Intensified Reaction and Separation Systems*. Annual Review of Chemical and Biomolecular Engineering, 2011. **2**(1): p. 431-451.
40. Jensen, K.F., *Flow chemistry—Microreaction technology comes of age*. AIChE Journal, 2017. **63**(3): p. 858-869.
41. Wang, K. and G. Luo, *Microflow extraction: A review of recent development*. Chemical Engineering Science, 2017. **169**: p. 18-33.

42. Dore, V., D. Tsaoulidis, and P. Angeli, *Mixing patterns in water plugs during water/ionic liquid segmented flow in microchannels*. Chemical Engineering Science, 2012. **80**: p. 334-341.
43. Li, Q. and P. Angeli, *Experimental and numerical hydrodynamic studies of ionic liquid-aqueous plug flow in small channels*. Chemical Engineering Journal, 2017. **328**: p. 717-736.
44. Jovanović, J., E.V. Rebrov, T.A. Nijhuis, M.T. Kreutzer, V. Hessel, and J.C. Schouten, *Liquid–Liquid Flow in a Capillary Microreactor: Hydrodynamic Flow Patterns and Extraction Performance*. Industrial & Engineering Chemistry Research, 2012. **51**(2): p. 1015-1026.
45. Angeli, P., E.G. Ortega, D. Tsaoulidis, and M. Earle, *Intensified Liquid-Liquid Extraction Technologies in Small Channels: A Review*. Johnson Matthey Technology Review, 2019. **63**(4): p. 299-310.
46. Matsuoka, A., K. Noishiki, and K. Mae, *Experimental study of the contribution of liquid film for liquid-liquid Taylor flow mass transfer in a microchannel*. Chemical Engineering Science, 2016. **155**: p. 306-313.
47. Kashid, M.N., Y.M. Harshe, and D.W. Agar, *Liquid–Liquid Slug Flow in a Capillary: An Alternative to Suspended Drop or Film Contactors*. Industrial & Engineering Chemistry Research, 2007. **46**(25): p. 8420-8430.
48. Tiwari, A., V.M. Rajesh, and S. Yadav, *Biodiesel production in micro-reactors: A review*. Energy for Sustainable Development, 2018. **43**: p. 143-161.
49. Pedersen, K.S., J. Imbrogno, J. Fonslet, M. Lusardi, K.F. Jensen, and F. Zhuravlev, *Liquid–liquid extraction in flow of the radioisotope titanium-45 for positron emission tomography applications*. Reaction Chemistry & Engineering, 2018. **3**(6): p. 898-904.
50. Kriel, F.H., G. Holzner, R.A. Grant, S. Woollam, J. Ralston, and C. Priest, *Microfluidic solvent extraction, stripping, and phase disengagement for high-value platinum chloride solutions*. Chemical Engineering Science, 2015. **138**: p. 827-833.
51. Tsaoulidis, D. and P. Angeli, *Effect of channel size on mass transfer during liquid–liquid plug flow in small scale extractors*. Chemical Engineering Journal, 2015. **262**: p. 785-793.
52. Juang, R.S. and Y.T. Chang, *Kinetics and mechanism for copper(II) extraction from sulfate solutions with bis(2-ethylhexyl)phosphoric acid*. Industrial & Engineering Chemistry Research, 1993. **32**(1): p. 207-213.
53. Teramoto, M., T. Yamashiro, A. Inoue, A. Yamamoto, H. Matsuyama, and Y. Miyake, *Extraction of amino acids by emulsion liquid membranes containing di (2-ethylhexyl)phosphoric acid as a carrier biotechnology; coupled, facilitated transport; diffusion*. Journal of Membrane Science, 1991. **58**(1): p. 11-32.
54. Itoh, H., M.P. Thien, T.A. Hatton, and D.I.C. Wang, *Water transport mechanism in liquid emulsion membrane process for the separation of amino acids*. Journal of Membrane Science, 1990. **51**(3): p. 309-322.
55. Tulasi, G.L. and S. Kumar, *Amino-acid extraction using D2EHPA: New description of equilibrium behavior*. AIChE Journal, 1999. **45**(12): p. 2534-2540.
56. *Chemistry of the Amino Acids*. Medical Journal of Australia, 1962. **2**(12): p. 469-469.
57. Biswas, R.K., R.A. Banu, and M.N. Islam, *Some physico-chemical properties of D2EHPA: Part 2. Distribution, dimerization and acid dissociation constants in n-hexane/1 M (Na+,H+)SO42– system, interfacial adsorption and excess properties*. Hydrometallurgy, 2003. **69**(1): p. 157-168.
58. Biswas, R.K., M.R. Zaman, and M.N. Islam, *Extraction of TiO2+ from 1 M (Na+, H+) SO42– by D2EHPA*. Hydrometallurgy, 2002. **63**(2): p. 159-169.
59. Nakamura, T., H. Terashima, and K. Mukai, *Emulsion formation and phase separation in some organic solvent-water systems. Mizu-abura kaimen ni okeru emulsion no seisei to sobunri*. Shigen To Sozai;(Japan), 1992. **108**(11).
60. Angeli, P. and A. Gavriilidis, *Hydrodynamics of Taylor flow in small channels: A Review*. Proceedings of the Institution of Mechanical Engineers, Part C: Journal of Mechanical Engineering Science, 2008. **222**(5): p. 737-751.

61. Suo, M. and P. Griffith, *Two-Phase Flow in Capillary Tubes*. Journal of Basic Engineering, 1964. **86**(3): p. 576-582.
62. Jovanović, J., W. Zhou, E.V. Rebrov, T.A. Nijhuis, V. Hessel, and J.C. Schouten, *Liquid–liquid slug flow: Hydrodynamics and pressure drop*. Chemical Engineering Science, 2011. **66**(1): p. 42-54.
63. Mac Giolla Eain, M., V. Egan, and J. Punch, *Film thickness measurements in liquid–liquid slug flow regimes*. International Journal of Heat and Fluid Flow, 2013. **44**: p. 515-523.
64. Tsaoulidis, D., E.G. Ortega, and P. Angeli, *Intensified extraction of uranium(VI) in impinging-jets contactors*. Chemical Engineering Journal, 2018. **342**: p. 251-259.
65. Torab-Mostaedi, M., A. Ghaemi, and M. Asadollahzadeh, *Prediction of mass transfer coefficients in a pulsed disc and doughnut extraction column*. The Canadian Journal of Chemical Engineering, 2012. **90**(6): p. 1570-1578.
66. Takahashi, K. and H. Takeuchi, *Interfacial Area of Liquid-Liquid Dispersion in a Mixer-Settler Extraction Column*, in *Process Metallurgy*, T. Sekine, Editor. 1992, Elsevier. p. 1357-1362.
67. Zhang, Q., L. Lin, and W. Ye, *Techniques for extraction and isolation of natural products: a comprehensive review*. Chinese Medicine, 2018. **13**(1): p. 20.
68. Skala, D. and V. Veljković, *Mass transfer characteristics in a gas-liquid reciprocating plate column. I. Liquid phase volumetric mass transfer coefficient*. The Canadian Journal of Chemical Engineering, 1988. **66**(2): p. 192-199.